

Stability Improvement of 60 GHz Narrowband Amplifier Using Microstrip Coupled Lines

Woojin Chang, Jong-Won Lim, Hokyun Ahn, Hong-Gu Ji, and Haecheon Kim

We present an analysis of microstrip coupled lines (MCLs) used to improve the stability of a 60 GHz narrowband amplifier. The circuit has a 4-stage structure implementing MCLs instead of metal-insulator-metal (MIM) capacitors for the unconditional stability of the amplifier and yield enhancement. The stability parameter, U , is used to compare the stability of MCLs with that of MIM capacitors. Experimental results show that MCLs are more stable than MIM capacitors with the same capacitances as MCLs because the parasitic parallel resistances of MCLs are lower than those of MIM capacitors. Moreover, the bandwidth of an amplifier using MCLs is narrower than one using MIM capacitors because the parasitic series inductances of MCLs are higher than those of MIM capacitors.

Keywords: 60 GHz amplifier, stability, microstrip coupled line, narrowband, millimeter-wave.

I. Introduction

In recent years, there has been major growth in millimeter-wave applications. There is a growing demand for support of 60 GHz systems, including wireless personal area networks (WPANs) and radio-over-fiber (RoF) systems. A 60 GHz RoF system has a narrow bandwidth of 59.6 GHz to 60.4 GHz. It needs the amplifiers to have a narrow bandwidth. In other words, some filters are needed to apply the broadband amplifiers to the narrowband system [1]. However, millimeter-wave filters incur some insertion loss and are expensive. We looked into some previous studies regarding a 60 GHz amplifier design and found an amplifier that shows an oscillation phenomenon [2]. To prevent such oscillation and enhance the stability of the amplifier, other methods have used resistors, negative feedback, or interstage mismatching [2]-[7]. The method using resistors improved the stability and prevented the oscillation of the amplifier [2]-[5]. However, this reduced the gain of the amplifier. Also, methods using negative feedback or interstage mismatching reduced the gain and increased the bandwidth of the amplifier. Therefore, we present an analysis of microstrip-coupled lines (MCLs) for designing narrowband millimeter-wave amplifiers and improving their stability to prevent an oscillation problem. A stability parameter is generally used for active devices, but in this paper, we expand the analysis to include passive devices in a search for more stability. We also propose a method for designing a narrowband amplifier to have more gain than amplifiers using previous methods, although they use the same active devices.

II. MCLs and MIM Capacitors

Figure 1 shows the general structures of the metal-insulator-

Manuscript received Apr. 28, 2009; revised July 1, 2009; accepted July 15, 2009.

This work was supported by the Ministry of Information and Communication, Rep. of Korea (project name: SoP for 60 GHz Pico-cell Communications).

Woojin Chang (phone: + 82 42 860 1270, email: wjchang@etri.re.kr), Jong-Won Lim (email: jwlim@etri.re.kr), Hokyun Ahn (email: hkahn@etri.re.kr), Hong-Gu Ji (email: hgji@etri.re.kr), and Haecheon Kim (email: khc@etri.re.kr) are with the Convergence Components & Material Research Laboratory, ETRI, Daejeon, Rep. of Korea.
doi:10.4218/etrij.09.1209.0012

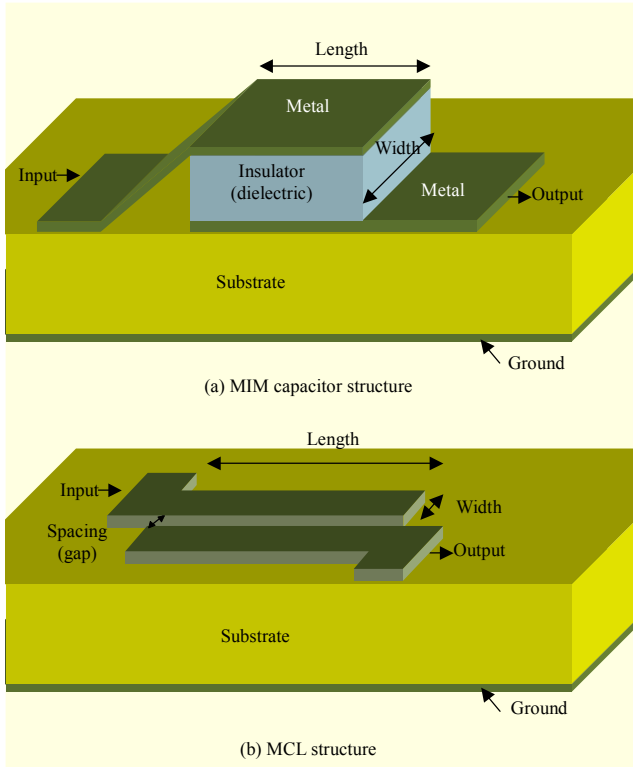


Fig. 1. Structures of the MIM capacitor and the MCL.

metal (MIM) capacitor and an MCL [8]. Their equivalent circuits are shown in Fig. 2 [9]. In this process, a silicon nitride thin film deposited by plasma enhanced chemical vapor deposition (PECVD) is used as a dielectric material in the MIM capacitor. The dielectric constant and DC resistivity of the silicon nitride are 7.5 and $10^{14} \Omega\text{-cm}$, respectively. The GaAs substrate has a thickness of $100 \mu\text{m}$ due to lapping for a backside via process, a dielectric constant of 12.9, and a dielectric loss tangent value of 0.001. Also, the metal characteristics of the microstrip and bias lines have a metal thickness of $3 \mu\text{m}$, metal bulk resistivity of $2.93 \mu\Omega\text{-cm}$, and a root-mean-square (RMS) surface roughness of 4 nm. In this process, the thickness of the silicon nitride is 980 \AA , and the capacitance per unit area of the MIM capacitors is $1 \text{ fF}/\mu\text{m}^2$. The MIM capacitors show about $\pm 10\%$ variation of their properties because of their dielectric constant and film thickness variations due to run-by-run fabrication. These variations degrade the RF circuit matching. A monolithic microwave integrated circuit (MMIC) is composed of active and passive devices, and the uniformity of each device in fabrication affects the yield. MCLs have lower variations in their characteristics compared to MIM capacitors because the effective metal thickness with 99% energy is very thin at millimeter-wave frequencies. Therefore, MCLs show very stable characteristics even if the metal thickness varies due to the run-by-run fabrication process.

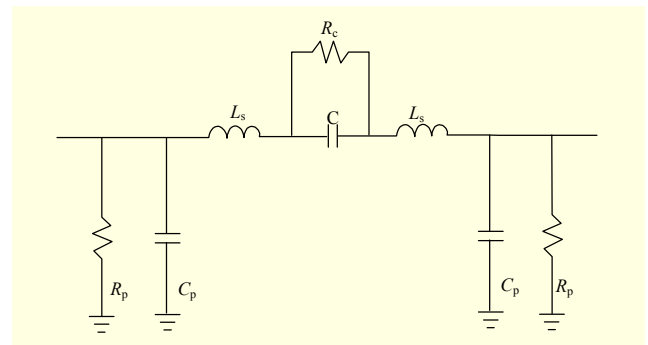


Fig. 2. Simplified equivalent circuit model for the MIM capacitor and the MCL.

The stability parameter is expressed as (1) and (2). The necessary and sufficient conditions for unconditional stability is $\mu > 1$ or $U > 0$. Larger values of μ or U imply greater stability [10], [11].

$$\mu = \frac{1 - |S_{11}|^2}{|S_{22} - S_{11}^*(S_{11}S_{22} - S_{12}S_{21})| + |S_{12}S_{21}|} > 1, \quad (1)$$

$$U = \mu - 1 = \frac{1 - |S_{11}|^2}{|S_{22} - S_{11}^*(S_{11}S_{22} - S_{12}S_{21})| + |S_{12}S_{21}|} - 1 > 0. \quad (2)$$

III. Analysis of MCLs and MIM Capacitors

Table 1 shows that the equivalent model values of the MCLs are comparable with those of MIM capacitors with the same capacitances (C). The values of the equivalent model parameters are extracted by fitting the equivalent model parameters with the S -parameters of the MCLs and MIM capacitors. The parasitic parallel resistance (R_p) and parasitic coupled resistance (R_c) of the MCLs are lower than those of the MIM capacitors, and the parasitic series inductance (L_s) and parasitic parallel capacitance (C_p) of the MCLs are higher than

Table 1. Extracted model parameters for the MIM capacitors and the MCLs.

	Size	C (fF)	R_c (k Ω)	L_s (pH)	C_p (fF)	R_p (k Ω)
MCL ($W=10 \mu\text{m}$, $S=10 \mu\text{m}$)	$52 \mu\text{m}$	4	23	68	6	111
	$116 \mu\text{m}$	9	11	100	11	48
	$192 \mu\text{m}$	16	7	124	17	24
	$260 \mu\text{m}$	25	4	128	23	14
MIM capacitor	$2 \times 2 \mu\text{m}^2$	4	740	1.1	0.07	57,200
	$3 \times 3 \mu\text{m}^2$	9	276	1.3	0.17	98,200
	$4 \times 4 \mu\text{m}^2$	16	152	2.0	0.18	97,400
	$5 \times 5 \mu\text{m}^2$	25	95	2.1	0.23	98,500

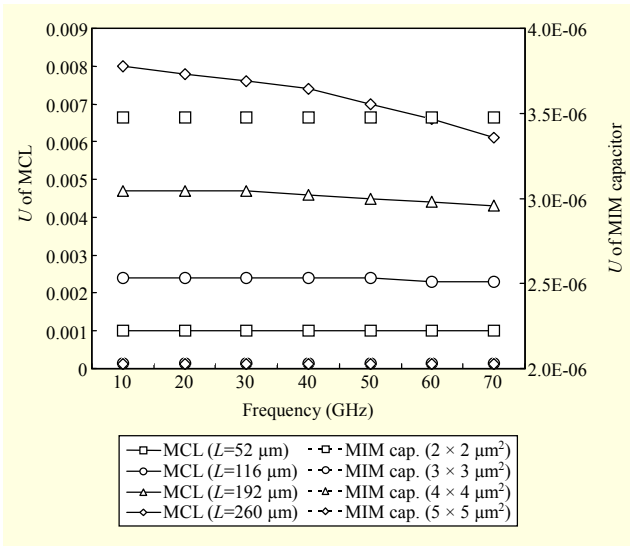


Fig. 3. Comparison of stability parameters (U) of the MIM capacitors and the MCLs.

those of the MIM capacitors as shown in Table 1.

Figure 3 compares the stability parameter, U , of the MCLs and MIM capacitors shown in Table 1. As shown in Fig. 3, the stability parameters of the MCLs are superior to those of the MIM capacitors for the various sizes shown. This significantly affects the stability of an amplifier. The stability of an amplifier with MCLs for the DC block and RF matching is more improved than those with MIM capacitors.

The equivalent circuit model of Fig. 2 was used to analyze the stability of the MIM capacitors and MCLs. To express the equivalent circuit model by its stability parameter, U , the equivalent circuit model converted Z_{12} and Z_{21} using (3).

$$Z_{12} = Z_{21} = \frac{R_c}{1 + j\omega R_c C} + 2j\omega L_s. \quad (3)$$

Then, Z_{12} and Z_{21} converted Y_{12} and Y_{21} using (4), and Y_{11} and Y_{22} were expressed in the equivalent circuit model parameters using (5).

$$Y_{12} = Y_{21} = -\frac{1}{Z_{12}}, \quad (4)$$

$$Y_{11} = Y_{22} = \frac{1}{R_p} + j\omega C_p - Y_{12}. \quad (5)$$

Next, the Y -parameters converted the S -parameters using (6) through (9).

$$S_{11} = \frac{(Y_0 - Y_{11})(Y_0 + Y_{22}) + Y_{12}Y_{21}}{(Y_0 + Y_{11})(Y_0 + Y_{22}) - Y_{12}Y_{21}}, \quad (6)$$

$$S_{12} = \frac{-2Y_{12}Y_0}{(Y_0 + Y_{11})(Y_0 + Y_{22}) - Y_{12}Y_{21}}, \quad (7)$$

$$S_{21} = \frac{-2Y_{21}Y_0}{(Y_0 + Y_{11})(Y_0 + Y_{22}) - Y_{12}Y_{21}}, \quad (8)$$

$$S_{22} = \frac{(Y_0 + Y_{11})(Y_0 - Y_{22}) + Y_{12}Y_{21}}{(Y_0 + Y_{11})(Y_0 + Y_{22}) - Y_{12}Y_{21}}. \quad (9)$$

Finally, the S -parameters converted U using (2). However, because the converted S -parameters were very complex, as shown in (6) through (9), U was too complex to discover its correlation with the equivalent model parameters using these equations. Therefore, we calculated U from the values of the extracted MIM capacitors and MCLs, shown in Table 1, using MATLAB.

Figure 4 shows a comparison between the stability of the parameters calculated from all model parameters of the MIM capacitor ($5 \mu\text{m} \times 5 \mu\text{m}$) and those calculated from one parameter from the MCL ($10 \mu\text{m} \times 10 \mu\text{m} \times 260 \mu\text{m}$) and the remaining parameters from the MIM capacitor ($5 \mu\text{m} \times 5 \mu\text{m}$). The graph shows that U is improved by R_p of the MCL. This means that the stability of the MCL is improved because it has a smaller parallel resistance than the MIM capacitor. However, it is revealed that the other model parameters cannot contribute toward improving the stability. Therefore, we can make a millimeter-wave amplifier that has more stability without resistors, negative feedback, or interstage mismatching. We can also obtain a higher amplifier gain with the MCLs than with the MIM capacitors.

Figure 5 shows the phases of the input reflection coefficient (S_{11}) for the MCLs and MIM capacitors. The phase change rates of the MCL frequencies are about 2 to 3 times higher than those of the MIM capacitors at 60 GHz. The phase change

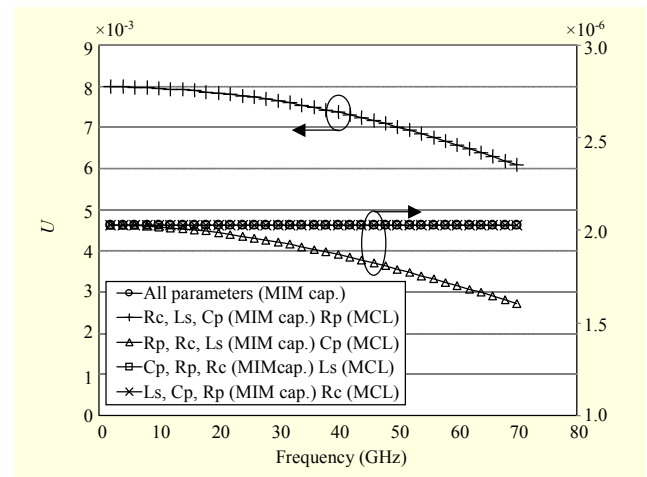


Fig. 4. Comparison of stability parameters calculated from all model parameters of the MIM capacitor ($5 \mu\text{m} \times 5 \mu\text{m}$) and those calculated from one parameter of the MCL ($10 \mu\text{m} \times 10 \mu\text{m} \times 260 \mu\text{m}$) and the rest of the MIM capacitor ($5 \mu\text{m} \times 5 \mu\text{m}$).

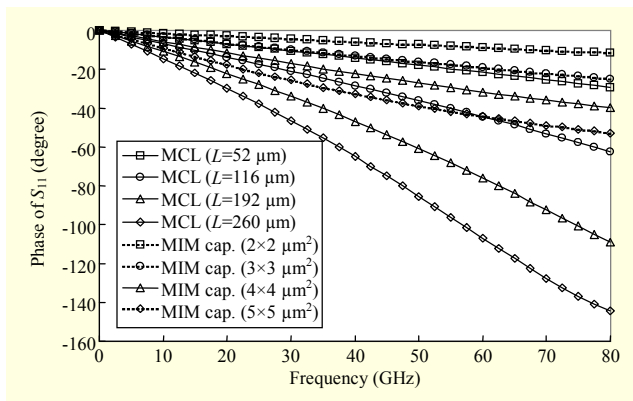


Fig. 5. Phases of S_{11} for the MCLs and the MIM capacitors.

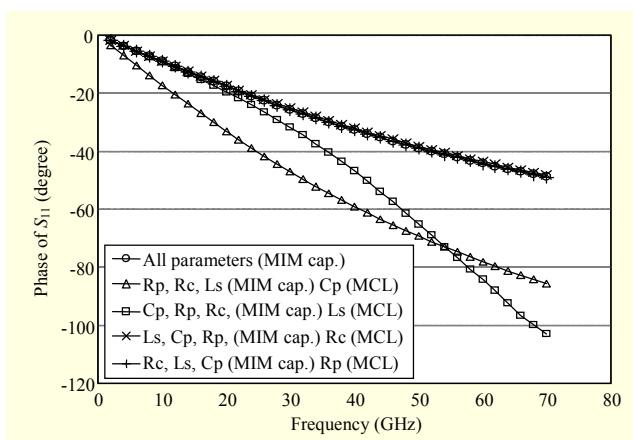


Fig. 6. Comparison of phases of the S_{11} calculated from all model parameters of the MIM capacitor ($5 \mu\text{m} \times 5 \mu\text{m}$) and those calculated from one parameter of the MCL ($10 \mu\text{m} \times 10 \mu\text{m} \times 260 \mu\text{m}$) and the rest of the MIM capacitor ($5 \mu\text{m} \times 5 \mu\text{m}$).

rates of the frequencies of passive devices have an influence on the bandwidth of the amplifier for matching circuits. Therefore, if the phase change rates of S_{11} of passive devices are high, the bandwidth of the amplifier for matching circuits narrows.

Figure 6 shows a comparison of the phases of S_{11} calculated from all model parameters of the MIM capacitor ($5 \mu\text{m} \times 5 \mu\text{m}$) and those calculated from one parameter from the MCL ($10 \mu\text{m} \times 10 \mu\text{m} \times 260 \mu\text{m}$) and the remaining parameters from the MIM capacitor ($5 \mu\text{m} \times 5 \mu\text{m}$). The phase change rates of the MIM capacitor ($5 \mu\text{m} \times 5 \mu\text{m}$) are 0.9 degree/GHz and 0.7 degree/GHz at 10 GHz and 60 GHz, respectively. Also, the phase change rates calculated from C_p of the MCL ($10 \mu\text{m} \times 10 \mu\text{m} \times 260 \mu\text{m}$) and the remaining parameters from the MIM capacitor ($5 \mu\text{m} \times 5 \mu\text{m}$) are 1.7 degree/GHz and 0.8 degree/GHz at 10 GHz and 60 GHz, respectively. It was revealed that the phase change rates of S_{11} at low frequencies increase due to C_p of the MCL. Also, the phase change rates calculated from L_s of the MCL ($10 \mu\text{m} \times 10 \mu\text{m} \times 260 \mu\text{m}$) and

the rest of the MIM capacitor ($5 \mu\text{m} \times 5 \mu\text{m}$) are 1.0 degree/GHz and 1.7 degree/GHz at 10 GHz and 60 GHz, respectively. It was revealed that the phase change rates of S_{11} at high frequencies increase due to L_s of the MCL. However, it was discovered that the other model parameters cannot influence the phase change rate of S_{11} . Therefore, we can make a millimeter-wave amplifier that has a narrow bandwidth using MCLs instead of MIM capacitors for matching circuits because they have a larger L_s than those of the MIM capacitors.

IV. Design of 60 GHz Amplifiers

The 60 GHz amplifiers were designed using a 4-inch $0.12 \mu\text{m}$ GaAs pseudomorphic high electron mobility transistor (PHEMT) process. The GaAs PHEMT has an effective gate length of $0.12 \mu\text{m}$, a unit gate width of $50 \mu\text{m}$, and two/four/eight gate fingers. The T-shaped gate of the PHEMT has a wide gate head of $1 \mu\text{m}$ and a gate foot of $0.12 \mu\text{m}$ [12], [13].

The PHEMT shows a peak transconductance ($G_{m,peak}$) of 500 mS/mm, a threshold voltage of -1.2 V , and a drain saturation current of 49 mA for 2 fingers, with a $100 \mu\text{m}$ total gate width ($2f100$) at $V_{ds} = 2 \text{ V}$. The RF characteristics of the PHEMT show a cutoff frequency, f_T , of 97 GHz, and a maximum oscillation frequency, f_{max} , of 166 GHz at $V_{ds} = 2 \text{ V}$ and $V_{gs} = -0.2 \text{ V}$.

A schematic of the 60 GHz amplifier using MIM capacitors and interstage mismatching, which is a conventional method for unconditional stability, is shown in Fig. 7. The amplifier was designed using a 4-stage structure with four $2f100$ s.

A schematic of the 60 GHz amplifier using MCLs instead of MIM capacitors, which is the proposed method for unconditional stability, is shown in Fig. 8. The amplifier was also designed using a 4-stage structure with four $2f100$ s for comparison with a 60 GHz amplifier using a conventional method.

This 60 GHz amplifier also uses NiCr thin-film resistors to provide high resistance on parts of the gate bias-lines to minimize RF signal leakage [14]. The matching points of the second and third stages of the four-stage amplifier are mismatched to achieve unconditional stability, just as in a conventional 60 GHz amplifier. The first and fourth stages of the four-stage amplifier have input/output matching. The MCLs in all interstages perform DC blocking and RF matching.

V. Measurements of 60 GHz Amplifiers

A microscopic view of the fabricated 60 GHz amplifier MMIC using MIM capacitors and interstage mismatching,

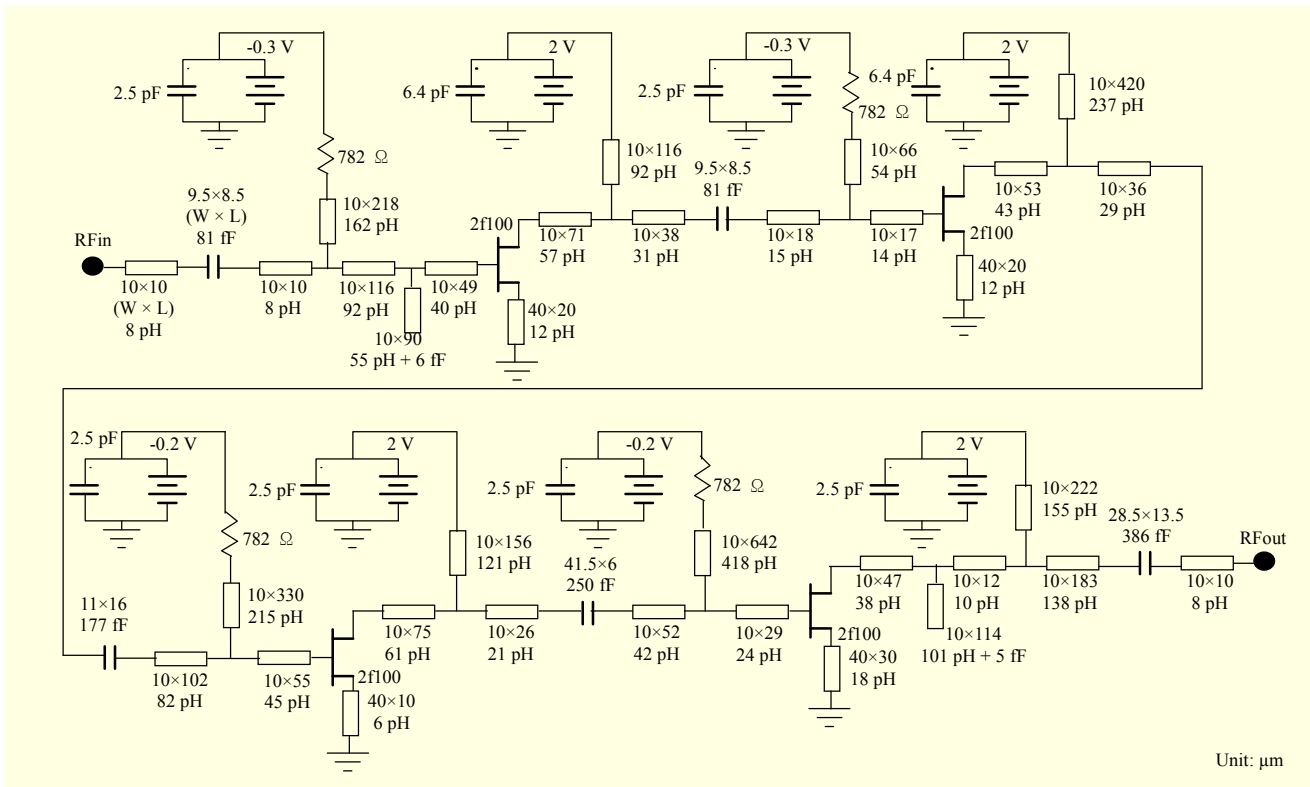


Fig. 7. Schematic of the 60 GHz amplifier using a conventional method.

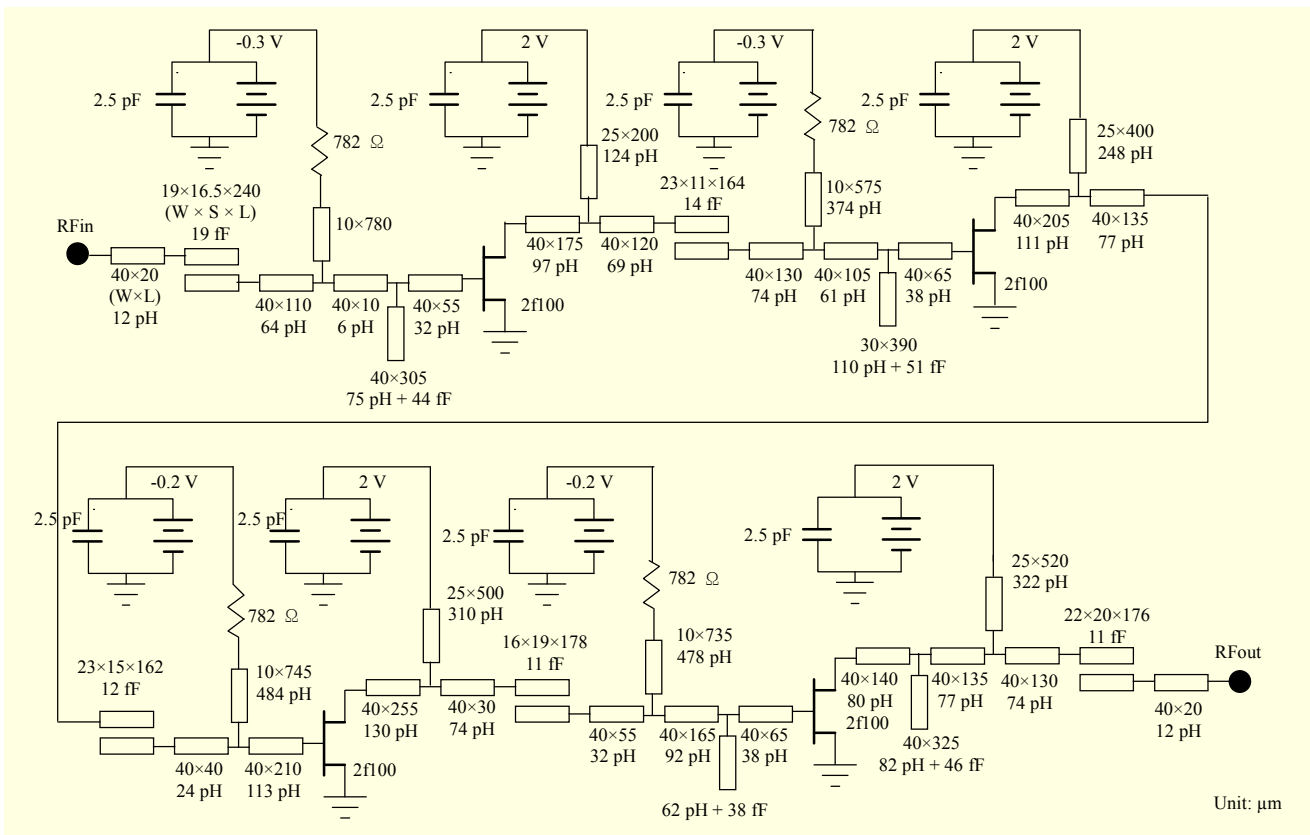


Fig. 8. Schematic of the 60 GHz amplifier using the proposed method.

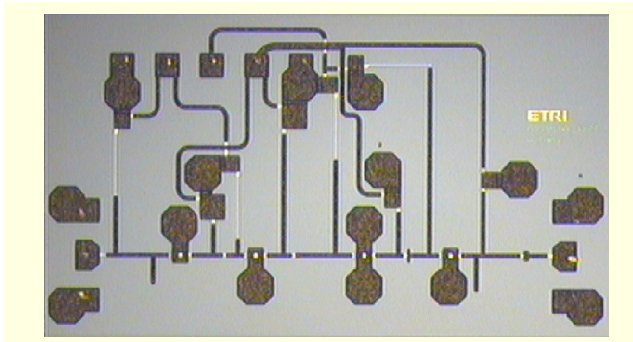


Fig. 9. Photograph of the fabricated 60 GHz amplifier MMIC using a conventional method.

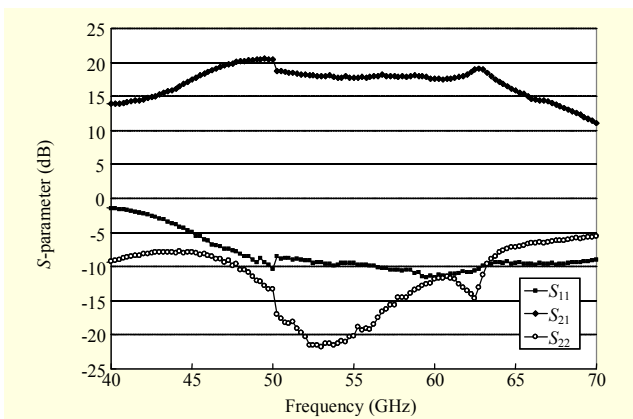


Fig. 10. Measured S -parameter of the fabricated 60 GHz amplifier MMIC using a conventional method.

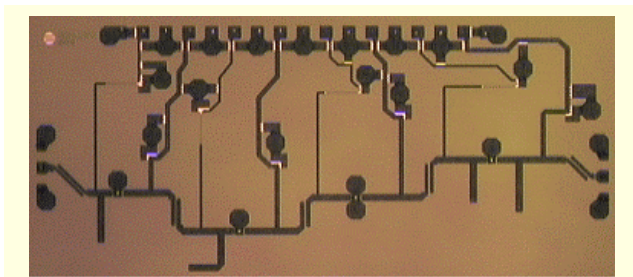


Fig. 11. Photograph of the fabricated 60 GHz amplifier MMIC using the proposed method.

which is a conventional method for unconditional stability, is shown in Fig. 9. The fabricated 60 GHz amplifier MMIC has a measured small signal gain (S_{21}) of 18 dB to 21 dB for 45.3 GHz to 63.8 GHz. It also has an S_{21} of 18 dB, an S_{11} of -12 dB to -11 dB, and an output reflection coefficient (S_{22}) of -13 dB to -12 dB for 59.5 GHz to 60.5 GHz as shown in Fig. 10.

A photograph of the fabricated 60 GHz amplifier MMIC using MCLs, which is the proposed method for improving stability, is shown in Fig. 11. The fabricated 60 GHz amplifier MMIC has a measured S_{21} of 21 dB to 24 dB for 58.5 GHz to 63.0 GHz. It also has an S_{21} of 22 dB, an S_{11} of -12 dB to

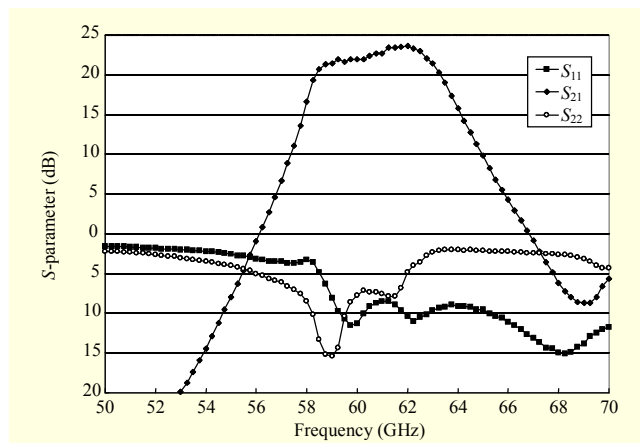


Fig. 12. Measured S -parameter of the fabricated 60 GHz amplifier MMIC using the proposed method.

Table 2. Summary of the performance of this work and the previously reported 60 GHz amplifiers.

	This work (proposed)	This work (conventional)	[15] (Finland)	[16] (Sweden)
Technology	0.12 μm GaAs PHEMT	0.12 μm GaAs PHEMT	0.1 μm GaAs PHEMT	0.15 μm GaAs PHEMT
Freq. (GHz)	58.5 to 63	45.3 to 63.8	50 to 65	50 to 65
3 dB bandwidth (GHz)	4.5	18.5	15.0	15.0
$BW_{3\text{ dB}}/F_{\text{center}}$ (%)	7.4	33.9	26.1	26.1
S_{21} (dB)	21 to 24	18 to 21	10.5 to 13.5	12 to 15
No. of stages	4	4	3	3
S_{21}/stage (dB)	5.3 to 6.0	4.5 to 5.3	3.5 to 4.5	4.0 to 5.0

-9 dB, and an S_{22} of -10 dB to -7 dB for 59.5 GHz to 60.5 GHz as shown in Fig. 12. The gain of the proposed amplifier is about 2.5 times better than that of a conventional amplifier using the same fabrication technology for 59.5 GHz to 60.5 GHz. The 3 dB bandwidths of the proposed amplifier and conventional amplifier are 4.5 GHz and 18.5 GHz, respectively.

Table 2 summarizes the performance of the 60 GHz amplifiers. The 3 dB bandwidth and gain of the proposed 60 GHz amplifier are narrower and better, respectively, than those of the conventional amplifier in this work and the amplifiers presented in [15] and [16].

VI. Conclusion

We present an analysis of MCLs for improving the stability of a 60 GHz narrowband amplifier for a 60 GHz RoF system with a bandwidth of 59.6 GHz to 60.4 GHz. The circuit has a

4-stage structure using MCLs instead of MIM capacitors for unconditional stability of the amplifier. We found that MCLs are more stable than MIM capacitors with the same capacitances because the parasitic parallel resistances of MCLs are lower than those of MIM capacitors. We also discovered that the bandwidth of an amplifier using MCLs is narrower than that of one using MIM capacitors because the parasitic series inductances of MCLs are higher than those of MIM capacitors. The proposed 60 GHz amplifier MMIC has a measured S_{21} of 21 dB to 24 dB for 58.5 GHz to 63.0 GHz. It also has an S_{21} of 22 dB, an S_{11} of -12 dB to -9 dB, and an S_{22} of -10 dB to -7 dB for 59.5 GHz to 60.5 GHz. The overall gain and gain per stage of the proposed amplifier are better than those of the conventional amplifier using the same fabrication technology. The 3 dB bandwidths of the proposed amplifier and conventional amplifier are 4.5 GHz and 18.5 GHz, respectively. Therefore, MCLs are considered to be applicable to improving the stability and narrowband performance characteristics of a millimeter-wave amplifier.

References

- [1] S. Kim et al., "High-Gain Wideband CMOS Low Noise Amplifier with Two-Stage Cascode and Simplified Chebychev Filter," *ETRI J.*, vol. 29, no. 5, Oct. 2007, pp. 670-672.
- [2] M. Karkkainen et al., "A Set of Integrated Circuits for 60 GHz Radio Front-End," *IEEE MTT-S Digest*, 2002, pp. 1273-1276.
- [3] T. Yao et al., "Algorithmic Design of CMOS LNAs and PAs for 60-GHz Radio," *IEEE J. Solid-State Circuits*, vol. 42, no. 5, May 2007, pp. 1044-1057.
- [4] Y. Mimino et al., "A 60 GHz Millimeter-Wave MMIC Chipset for Broadband Wireless Access System Front-End," *IEEE MTT-S Digest*, 2002, pp. 1721-1724.
- [5] H. Zirath et al., "Development of 60 GHz Front End Circuits for High Data Rate Communication System in Sweden and Europe," *IEEE GaAs Digest*, 2003, pp. 93-96.
- [6] H. Zirath et al., "Development of 60-GHz Front-End Circuits for High-Data-Rate Communication System," *IEEE J. Solid-State Circuits*, vol. 39, no. 104, Oct. 2004, pp. 1640-1649.
- [7] M. Varonen et al., "Power Amplifier for 60 GHz WPAN Applications," *Radio and Wireless Conf. Digest*, Aug. 2002, pp. 11-14.
- [8] K.C. Gupta et al., *Microstrip Lines and Slotlines*, 2nd Ed., Artech House, 1996.
- [9] J.P. Mondal, "An Experimental Verification of a Simple Distributed Model of MIM Capacitors for MMIC Applications," *IEEE Trans. MTT*, vol. 35, no. 4, Apr. 1987, pp. 403-408.
- [10] M.L. Edwards et al., "A New Criterion for Linear 2-Port Stability Using a Single Geometrically Derived Parameter," *IEEE Trans. MTT*, vol. 43, no. 12, Dec. 1992, pp. 2303-2311.
- [11] D.M. Pozar, *Microwave Engineering*, 2nd Ed., John Wiley & Sons, 1981.
- [12] J.W. Lim et al., "0.12 um Gate Length T-Shaped AlGaAs/InGaAs/GaAs Pseudomorphic High-Electron-Mobility Transistors Fabricated Using a Plasma-Enhanced Chemical Vapor Deposited Silicon-Nitride-Assisted Process," *Jpn. J. Appl. Physics*, vol. 43, no. 12, Dec. 2004, pp. 7934-7938.
- [13] W. Chang et al., "A 60 GHz Medium Power Amplifier for Radio-over-Fiber System," *ETRI J.*, vol. 29, no. 5, Oct. 2007, pp. 673-675.
- [14] Y. Lee et al., "Highly Linear and Efficient Microwave GaN HEMT Doherty Amplifier for WCDMA," *ETRI J.*, vol. 30, no. 1, Feb. 2008, pp. 158-160.
- [15] Mikko Varonen et al., "Integrated Power Amplifier for 60 GHz Wireless Applications," *IEEE MTT-S Digest*, 2003, pp. 915-918.
- [16] S.E. Gunnarsson et al., "Highly Integrated 60 GHz Transmitter and Receiver MMICs in a GaAs pHEMT Technology," *IEEE J. Solid-State Circuits*, vol. 40, no. 11, Nov. 2005, pp. 2174-2186.



Woojin Chang received the BS and MS degrees in information engineering from Korea University, Korea, in 1996 and 1998, respectively, and the PhD degree in electronic engineering from Chungnam National University, Korea, in 2008. From 1998 to 1999, he worked as an engineer with LG Precision Co.

Ltd., Korea, where he was engaged in the research and development of power amplifier modules for wireless communications. In 1999, he joined ETRI, Korea, where he is currently a senior engineer. His research interests include design and analysis of power amplifiers, low noise amplifiers, and mixer MMICs operating up to the millimeter-wave range, as well as active and passive components modeling.

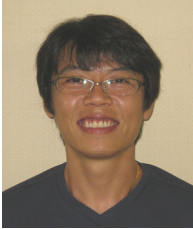


Jong-Won Lim received the BS, MS, and PhD degrees in physics from Chung-Ang University in Seoul, Korea, in 1988, 1990, and 1998, respectively. In 1998, he joined ETRI of Korea, as a senior member of research staff, where he has been engaged in research on compound semiconductor MMIC development for wireless telecommunications. His recent research involves the development of 50 nm InP HEMT technology in THz frequency range.



Hokyun Ahn received the BS and MS degrees in material science and engineering from Korea University, Korea, in 1999 and 2001, respectively. He joined ETRI in 2001. Since 2001, he has been involved in developing an e-beam lithography process and fabrication processes of compound semiconductor devices

such as GaAs, InP, and GaN related devices. He is now a senior member of engineering staff with the Photonic/Wireless Convergence Components Research Department of ETRI.



Hong-Gu Ji received the BS and MS degrees in radio science and engineering from Kwangwoon University, Seoul, Korea, in 1998 and 2000, respectively. He joined ETRI in 2000. Since 2000, he has been involved in design and measurement MMICs of compound

semiconductors, such as GaAs, InP, and SiGe related devices. He is now a senior member of engineering staff with the Photonic/Wireless Convergence Components Research Department of ETRI.



Haecheon Kim received the BS degree in metallurgical engineering from Seoul National University in 1982 and the MS degree in materials science and engineering from Korea Advanced Institute of Science and Technology (KAIST), Seoul, Korea, in 1984. He earned the PhD degree in materials science and

engineering from Illinois Institute of Technology (IIT) in Chicago, USA, in 1992. From 1984 to 1988, he was with LG Electronics, as a senior research member of the Central Research Center, where he was engaged in R&D on magnetic materials for 8 mm video tape and thin film transistors for LCD panels. In 1993, he joined ETRI of Korea, as a senior member of research staff of the Compound Semiconductor Department. He is currently leading the Microwave Convergence Devices Team. His research interests are in GaAs/InP/GaN devices, MMICs, and their system applications.